Directed HK propagator

Lucas Kocia and Eric J. Heller

Citation: The Journal of Chemical Physics **143**, 124102 (2015); doi: 10.1063/1.4931406
View online: http://dx.doi.org/10.1063/1.4931406
View Table of Contents: http://scitation.aip.org/content/aip/journal/jcp/143/12?ver=pdfcov
Published by the AIP Publishing

Directed HK propagator

Lucas Kocia[1,a)] and Eric J. Heller[1,2]
[1]*Department of Chemistry and Chemical Biology, Harvard University, Cambridge, Massachusetts 02138, USA*
[2]*Department of Physics, and Department of Chemistry and Chemical Biology, Harvard University, Cambridge, Massachusetts 02138, USA*

(Received 16 March 2015; accepted 9 September 2015; published online 22 September 2015)

We offer a more formal justification for the successes of our recently communicated "directed Heller-Herman-Kluk-Kay" (DHK) time propagator by examining its performance in one-dimensional bound systems which exhibit at least quasi-periodic motion. DHK is distinguished by its single one-dimensional integral—a vast simplification over the usual $2N$-dimensional integral in full Heller-Herman-Kluk-Kay (for an N-dimensional system). We find that DHK accurately captures particular coherent state autocorrelations when its single integral is chosen to lie along these states' fastest growing manifold, as long as it is not perpendicular to their action gradient. Moreover, the larger the action gradient, the better DHK will perform. We numerically examine DHK's accuracy in a one-dimensional quartic oscillator and illustrate that these conditions are frequently satisfied such that the method performs well. This lends some explanation for why DHK frequently seems to work so well and suggests that it may be applicable to systems exhibiting quite strong anharmonicity. © *2015 AIP Publishing LLC.* [http://dx.doi.org/10.1063/1.4931406]

INTRODUCTION

Semiclassical methods for quantum time propagation aspire to accomplish propagation of states as faithfully as possible with as few resources as necessary. Frequently, due to their classical underpinnings, they also yield invaluable physical insight behind the phenomenon they are modeling. The earliest formulation of such a method was the well-known van Vleck-Morette-Gutzwiller (VVMG) propagator. Today, perhaps the most popular variant of the VVMG is the Heller-Herman-Kluk-Kay (HK) propagator,[1–4] a uniformization of VVMG expressed in so-called initial value representation. Unfortunately, despite many efforts, HK has seldom been found to be computationally feasible in systems with dimension greater than ten. This is largely due to the prohibitive cost of computing the stability matrix elements associated with the trajectories that contribute to its uniformizing integral. Not only does the dimension of these matrix elements increase with the number of degrees of freedom of the system but the number of trajectories necessary for convergence also tends to proliferate.

Efforts to alleviate this problem have frequently found some effect, especially in chaotic systems. These include cellular dephasing,[5] Filinov filtering,[6] and throwing out divergent trajectories.[7] However, these methods have proven ineffective in many other systems and only reduce the growth of trajectories necessary to a point.[8] There has been some work modifying the Filinov filtering approach such that it differs in the different directions associated with HK's stability matrices.[9] The method presented herein is similar in spirit to this approach.

The classical dynamics of bound systems frequently exhibit anisotropic spreading in phase space which can be taken advantage of to perform uniformization more quickly and cleverly. We present here a more thorough examination of a method, called the "directed Heller-Herman-Kluk-Kay" (DHK) propagator, that exploits this phenomenon and which we introduced in a recent Communication.[10] DHK contains only a single integral whose domain is chosen to lie along a one-dimensional manifold selected from the classical dynamics of the state of interest. In our earlier work, we showed that it is frequently able to approach exact quantum results even though it only requires a fraction of the computational cost of HK. In particular, DHK was effective at obtaining eigenspectra in anharmonic systems with up to six coupled degrees of freedom. Here, we explore how this was possible in a simpler one-dimensional (two dimensions in phase space) setting.

MOTIVATION

In hyperbolic systems, there exist stable and unstable manifolds which characterize all trajectories. Those on the unstable manifold will exponentially depart from a fixed point while trajectories on the stable manifold will exponentially approach a fixed point. Though most bound systems cannot be characterized in this way, they frequently still exhibit at least quasi-periodic points around which growing and compressing manifolds can be found (as long as the potential has some anharmonicity). An example is shown in the inset of Fig. 1 where the phase space of a quartic oscillator is shown and the trajectories making up the density of an initial coherent state stretch out along the manifold delineated by the green curve after it has undergone one period.

[a)]Author to whom correspondence should be addressed. Electronic mail: lkocia@fas.harvard.edu.

In this paper, we consider the dynamics of quantum states that are initially coherent states. The diagonal term for the HK propagator in a coherent state representation (equivalently the autocorrelation of a coherent state) is

$$\langle\Psi_\beta(0)|\Psi_\beta(t)\rangle_{\mathrm{HK}} = \left(\frac{\sqrt{\gamma\gamma_\beta}}{\pi\hbar\left(\gamma+\gamma_\beta\right)}\right)^N \int \mathrm{d}\boldsymbol{p}_0 \int \mathrm{d}\boldsymbol{q}_0 C_t(\boldsymbol{p}_0,\boldsymbol{q}_0)\exp\left[\frac{i}{\hbar}S_t(\boldsymbol{p}_0,\boldsymbol{q}_0)\right] g_\beta(\boldsymbol{p}_0,\boldsymbol{q}_0)g_\beta^*(\boldsymbol{p}_t,\boldsymbol{q}_t), \tag{1}$$

where

$$g_\beta(\boldsymbol{p},\boldsymbol{q}) = \exp\left[-\frac{\gamma_\beta\gamma}{2(\gamma+\gamma_\beta)}(\boldsymbol{q}-\boldsymbol{q}_\beta)^2 - \frac{1}{2\hbar^2(\gamma+\gamma_\beta)}(\boldsymbol{p}-\boldsymbol{p}_\beta)^2 + \frac{i}{\hbar(\gamma+\gamma_\beta)}(\boldsymbol{q}-\boldsymbol{q}_\beta)\cdot(\gamma\boldsymbol{p}_\beta+\gamma_\beta\boldsymbol{p})\right], \tag{2}$$

and the preexponential is

$$C_t(\boldsymbol{p}_0,\boldsymbol{q}_0) = \sqrt{\det\left[\frac{1}{2}\left(\frac{\partial\boldsymbol{p}_t}{\partial\boldsymbol{p}_0}+\frac{\partial\boldsymbol{q}_t}{\partial\boldsymbol{q}_0}-i\hbar\gamma\frac{\partial\boldsymbol{q}_t}{\partial\boldsymbol{p}_0}+\frac{i}{\hbar\gamma}\frac{\partial\boldsymbol{p}_t}{\partial\boldsymbol{q}_0}\right)\right]}. \tag{3}$$

This term contains elements of the stability matrix

$$\boldsymbol{M}(t) = \begin{pmatrix}\boldsymbol{M}(t)_{11} & \boldsymbol{M}(t)_{12}\\ \boldsymbol{M}(t)_{21} & \boldsymbol{M}(t)_{22}\end{pmatrix} = \begin{pmatrix}\left(\frac{\partial\boldsymbol{p}_t}{\partial\boldsymbol{p}_0}\right)_{\boldsymbol{q}_0} & \left(\frac{\partial\boldsymbol{p}_t}{\partial\boldsymbol{q}_0}\right)_{\boldsymbol{p}_0}\\ \left(\frac{\partial\boldsymbol{q}_t}{\partial\boldsymbol{p}_0}\right)_{\boldsymbol{q}_0} & \left(\frac{\partial\boldsymbol{q}_t}{\partial\boldsymbol{q}_0}\right)_{\boldsymbol{p}_0}\end{pmatrix}. \tag{4}$$

Vectors are denoted by lowercase bold letters while matrices are denoted by uppercase bold letters (e.g., $\boldsymbol{a}$ and $\boldsymbol{A}$, respectively). The coherent state Ψ_β has dispersion γ_β whereas γ are those of the "frozen" coherent states centered at $(\boldsymbol{p}_0,\boldsymbol{q}_0)$ whose overlaps with $\Psi_\beta(0)$ and $\Psi_\beta(t)$, $g_\beta(\boldsymbol{p}_0,\boldsymbol{q}_0)g_\beta^*(\boldsymbol{p}_t,\boldsymbol{q}_t)$, are integrated over. Each frozen state is governed by its central classical trajectory with associated actions S_t and stability matrices $\boldsymbol{M}(t)$ that are both accounted for through the phase and preexponential terms, respectively.

As can be seen in Eqs. (1)–(3), HK has several ingredients: (a) the actual overlap between the initial and propagated coherent states as sampled by "frozen" coherent states, (b) the phase due to their action, and the (c) phase and (d) magnitude of their preexponential involving stability matrix elements. Figure 2 shows how all of these vary along the green manifold in a quartic oscillator system for states labeled A, B, C, and D. Forecasting the effectiveness of DHK, it can be seen that this manifold cuts through and samples a good average of all the ingredients in the area of highest overlap for every state except C. Furthermore, the phase space densities of the states asymptotically approach the manifold with time. In this way, it can be seen that integrating along it may proportionally represent all adjacent phase space points appropriately and so render their explicit inclusion through a larger dimensional integral such as HK's unnecessary. DHK exploits this idea, and as the right column of Fig. 2 (as well as Fig. 1) shows, its autocorrelations can be in very good agreement with HK's.

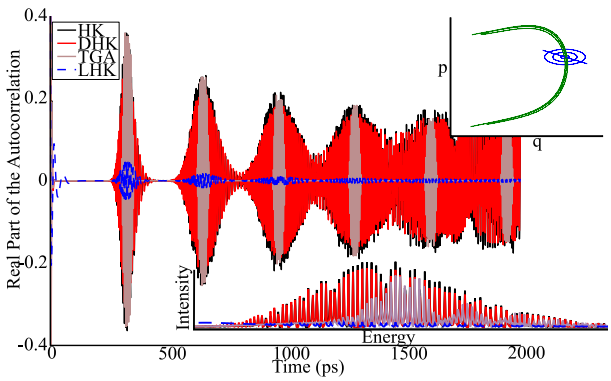

FIG. 1. The real part of the autocorrelation compared between HK, DHK, TGA, and LHK. TGA is the thawed Gaussian approximation.[11] Inset, top-right: the phase space overlap between the initial (blue) and time evolved (green) coherent state. The blue line corresponds to the manifold over which DHK's integral was evaluated. Inset, bottom-right: the Fourier transform of the autocorrelation.

FORMULATION OF DHK

DHK replaces HK's full $2N$-dimensional integral with one along a selected one-dimensional manifold $\mathcal{L}$, which can differ from any of the $2N$ integral domains of the full HK expression,

$$\begin{aligned}\langle\Psi_\beta(0)|\Psi_\beta(t)\rangle_{\mathrm{HK}} &= \int_{-\infty}^{\infty}\mathrm{d}^{2N}\boldsymbol{x}_0\xi(\boldsymbol{x}_0,t) \approx \mathcal{N}^{-1}\int_{\mathcal{L}}\mathrm{d}l\,\xi(\boldsymbol{x}_0(l),t)\\ &\equiv \langle\Psi_\beta(0)|\Psi_\beta(t)\rangle_{\mathrm{DHK}},\end{aligned} \tag{5}$$

where ξ is the integrand in the full HK formula. Naturally, we desire such a method to still be normalized such that it is 1 at $t = 0$. This means that

$$\mathcal{N} = \int_{\mathcal{L}}\mathrm{d}l\,\xi(\boldsymbol{x}_0(l),0). \tag{6}$$

It is therefore necessary in any application of Eq. (5) to show that there exists such a manifold $\mathcal{L}$, which is a good representation of the full HK integral's domain. To accomplish this, it is important to examine the "ingredients" of HK's integrand ξ where it is most significant, namely, for the autocorrelation examined here, in the phase space region of the initial coherent state.

A cursory examination of recurrences in phase space (such as in Fig. 2) reveals that the phase due to the evolved state's action is often the most significantly varying component of ξ on the scale of the area of overlap with the initial state when compared with the magnitude and phase of the associated preexponential. This is reasonable since the preexponential is a function of the stability matrices of the underlying trajectories and is responsible for preserving HK's norm; it will only vary between areas in phase space that are experiencing different environments of compression and stretching and this generally occurs at scales that are larger than that of the area of the initial coherent state. The phase change from the action along

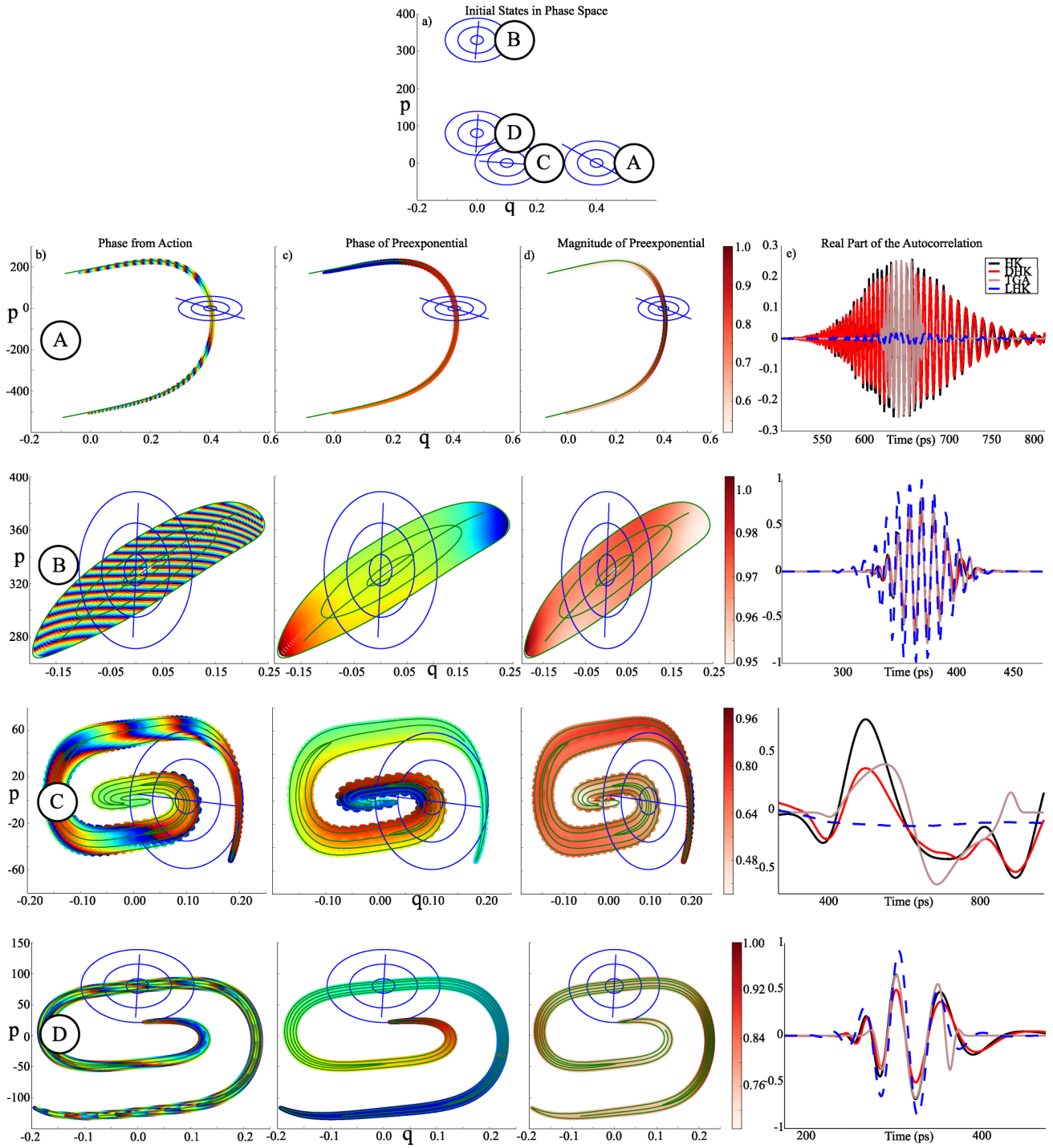

FIG. 2. (a) The initial phase space distributions of the four coherent states A-D in the quartic oscillator system investigated are shown. Organized column-wise are plots of each state's (b) phase due to its action, and (c) phase and (d) magnitude of its HK preexponential immediately after one orbit. Also shown are the corresponding (e) first recurrences of their autocorrelations. The blue line corresponds to the manifold over which DHK's integral was evaluated which evolves into the green line after one orbit. Integrating along this manifold is intended to proportionally represent the rest of the overlap phase space. Shown superimposed on the plots in (a)-(d) are corresponding concentric initial (blue) and final (green) confidence intervals of the underlying wavefunction density.

a manifold with endpoints l_1 and l_2,

$$S(\boldsymbol{p}_0(l_2),\boldsymbol{q}_0(l_2),t) - S(\boldsymbol{p}_0(l_1),\boldsymbol{q}_0(l_1),t) = \int_{q_t(l_1)}^{q_t(l_2)} \boldsymbol{p}\cdot \mathrm{d}\boldsymbol{q}, \qquad (7)$$

can vary far more quickly.

Therefore, when examining the largest contributions to the characteristics of ξ, it is often sufficient to only consider the density of the overlap and the phase from the action at the point of largest overlap. In particular, we proceed to approximate the overlap of the time propagated coherent state $\Psi_\beta(t)$ with its initial self $\Psi_\beta(0)$, by representing both by Gaussians $\Psi_\beta(q,t) \approx \left(\frac{\Re\gamma_t}{\pi}\right)^{\frac{1}{4}} \exp\left[-\frac{\gamma_t}{2}(q-q_\beta^2) + \frac{i}{\hbar}p_\beta(q-q_\beta)\right]$ (though the propagated state will no longer be a Gaussian in anharmonic systems) and consider their respective Wigner functions,

$$\rho_W(p,q,\theta,\gamma) = \frac{1}{\pi\hbar}\exp\left\{[(p-p_\beta,q-q_\beta)\cdot R(\theta)]\begin{pmatrix}-\frac{1}{\gamma\hbar^2} & 0\\ 0 & -\gamma\end{pmatrix}[(p-p_\beta,q-q_\beta)\cdot R(\theta)]^T\right\}, \tag{8}$$

where θ denotes their rotation with respect to the origin, γ are their dispersions along their major and minor axes ($\gamma = \frac{\sin\theta + i\gamma_t\hbar\cos\theta}{\gamma_t\hbar^2\sin\theta + i\hbar\cos\theta} \in \mathbb{R}$, not to be confused with the γ of HK's frozen sampling Gaussians, g_β, discussed in the Motivation), and $R(\theta)$ is the standard 2×2 rotation matrix. See the Appendix for a derivation. These Gaussian fits of $\Psi_\beta(t)$ are equivalent to its propagation under a harmonic expansion of the potential at its center in phase space (such as in the thawed Gaussian approximation[11]). We further approximate the contribution of the phase from the action via a plane wave

$$\exp\left[ik(\cos(\phi)\hat{p} - \sin(\phi)\hat{q})\cdot(p,q)^T/\hbar\right], \tag{9}$$

which is rotated by ϕ with respect to the $\hat{p}$ axis and has momentum k. The top-right of Fig. 3 illustrates how these approximate the overlap and phase of a particular recurrence.

Under these approximations, the full HK autocorrelation at a point in time during a recurrence corresponds to taking the full integral of the two ρ_Ws, with one rotated by θ compared to the other, all modulated by the plane wave,

$$O_{\mathrm{HK}}(t) \approx \int_{-\infty}^{\infty}\mathrm{d}p\int_{-\infty}^{\infty}\mathrm{d}q\,\rho_W(p,q;0,\gamma_0)\rho_W(p,q;\theta,\gamma) \times \exp\left[ik(\cos(\phi)\hat{p} - \sin(\phi)\hat{q})\cdot(p,q)^T/\hbar\right]. \tag{10}$$

We let the fastest growing manifold lie along the p-coordinate cutting through the center of the coherent state so that its stretching in this direction is proportional to γ. It follows that $\theta \approx 0$ in the limit that the dynamics are wholly linearizable. Therefore, if we set DHK's $\mathcal{L}$ manifold to lie along the state's fastest growing manifold—which seems sensible since such an $\mathcal{L}$ will contribute non-zero overlaps for the appropriate times as the state passes through a recurrence—DHK will correspond to a simplified version of Eq. (10),

$$O_{\mathrm{DHK}}(t) \approx \frac{\int_{-\infty}^{\infty}\mathrm{d}l\,\rho_W(l,0;0,\gamma_0)\rho_W(l,0;0,\gamma)\exp\left[ik(\cos(\phi)\hat{p} - \sin(\phi)\hat{q})\cdot(p,q)^T/\hbar\right]}{\int_{-\infty}^{\infty}\mathrm{d}l\,\rho_W(l,0;0,\gamma_0)\rho_W(l,0;0,\gamma_0)}. \tag{11}$$

We are interested in the absolute value of the difference of $O_{\mathrm{DHK}}(t)$ and O_{HK}, a measure of the expected error in DHK, where $\theta \approx 0$,

$$|O_{\mathrm{DHK}}(t) - O_{\mathrm{HK}}(t)| = \left|\sqrt{\frac{2\gamma}{\gamma+\gamma_0}}e^{-\frac{\gamma\gamma_0 k^2\cos^2(\phi)}{4(\gamma+\gamma_0)}} - \frac{2\sqrt{\gamma\gamma_0}}{\gamma+\gamma_0}e^{-\frac{k^2((\gamma\gamma_0-1)\cos(2\phi)+\gamma\gamma_0+1)}{8(\gamma+\gamma_0)}}\right|. \tag{12}$$

An examination of this error shown in Fig. 3 reveals that, under the aforementioned approximations of the modeled overlap, DHK always approaches HK's value for all k and ϕ when $\frac{\gamma}{\gamma_0} \ll 1$, where γ_0 is the dispersion of the initial coherent state and γ is its dispersion during the recurrence along the (fastest growing) manifold sampled. The greater the manifold's growth, the larger the γ is. This may seem troubling, since it means that accuracy of DHK is only ensured when its one-dimensional integral is performed along the direction that has shrunk, not grown, and such a manifold would only capture the middle of recurrences well when the center of the state has returned near its initial point. However, all is saved by non-zero phase variation from action; in particular, Fig. 3 shows that when DHK's integral lies along the fastest growing manifold ($\gamma > \gamma_0$), its agreement with HK improves the larger the wavevector k of the plane wave is and as long as ϕ, its angle, is not perpendicular to this manifold. This last requirement is likely due to the fact that sampling along $\mathcal{L}$ when it lies perpendicular to the gradient of action would only include one value of this variation and thus hardly serve as its representative average.

Substituting in the appropriate angles ϕ of the momentum k found at the moment of the first recurrence of states $A-D$ into Eqs. (10) and (11) reveals that they all satisfy this last requirement of $\phi \neq \pi/2$ and so lie in areas where DHK is close to HK's value, except for C, as indicated by the markers in Fig. 3. For state C, the gradient of action varies perpendicular to the major axis of its initial and final states. C's initial dispersion γ_0 is too small for DHK to handle this perpendicular angle of action variation $\phi = \pi/2$. This agrees well with the relatively poorer autocorrelation calculated from DHK for system C seen in Fig. 2(e).

We have so far illustrated that it is often quite reasonable to assume, in bound anharmonic systems exhibiting at least quasi-periodicity, that recurrences which can be well described by our simple Gaussian-plane wave model can frequently be well approximated by only the single integral in Eq. (5) when $\mathcal{L}$ is chosen to lie along the fastest growing manifold of the coherent state.

Linearizing around such a chosen manifold $\mathcal{L}$ (by Taylor expanding) is an approach that may appear to be closely related, at least at first glance. Its derivation is presented in the

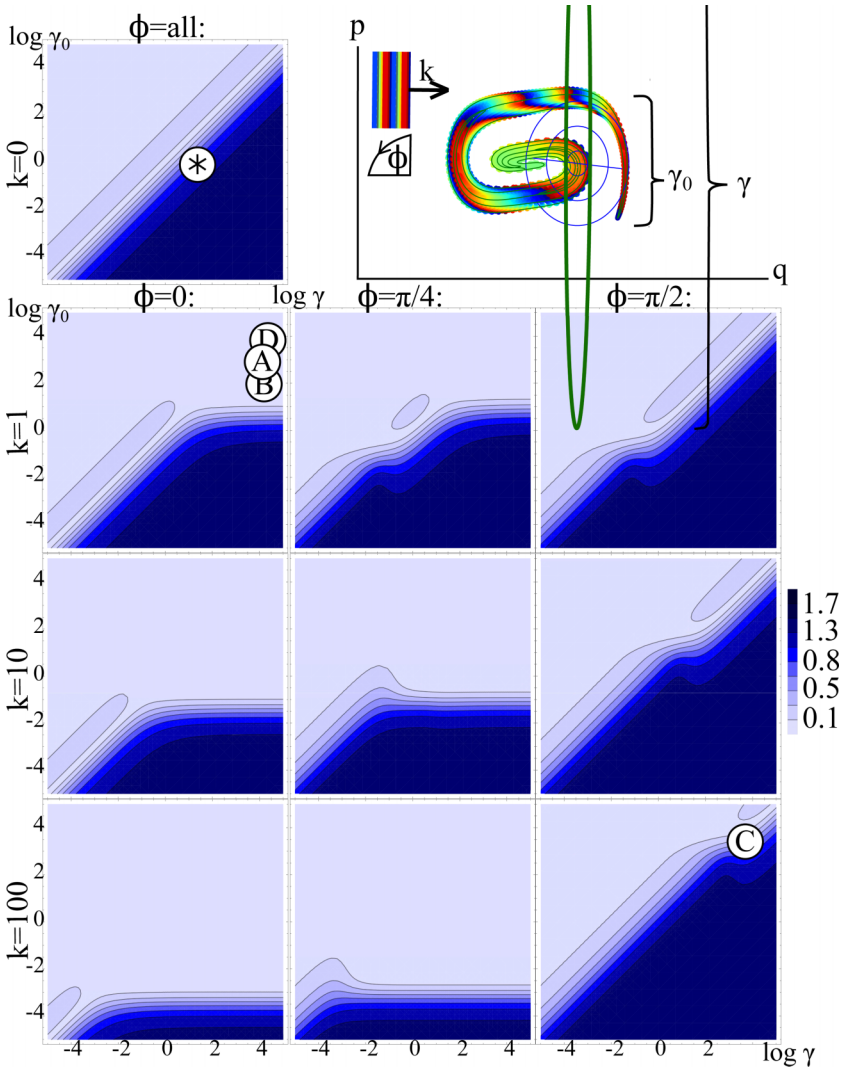

FIG. 3. The contour plots for various values of k and ϕ of $|O_{\mathrm{DHK}}(t) - O_{\mathrm{HK}}(t)|$ defined by Eqs. (10) and (11). These indicate that when $\mathcal{L}$ lies along the fastest growing manifold, DHK fares best at reproducing autocorrelations when $\frac{\gamma}{\gamma_0} \ll 1$ but also will agree with HK better the larger k is as long as $\phi \neq \pi/2$. In other words, DHK will be more accurate the greater the gradient of the action as long as it does not face perpendicularly to $\mathcal{L}$. This means that the first recurrence of system A, B, and D (shown in white markers) should be well treated by DHK. C's first recurrence should be less accurately captured. This qualitatively agrees with the results shown in Fig. 2(e). Note that representing A's phase of action by a plane wave is a rather poor approximation as can be seen in Fig. 2, however its wavevector in the vicinity of the overlap is $k > 0$ and $\phi \approx 0$.

Appendix. The autocorrelations of the resultant method, which we refer to herein as "linearized HK" (LHK), are compared to DHK in Fig. 2(e) and are shown to often be inferior to DHK in the quartic system examined. This can be explained by noting that DHK's manifold $\mathcal{L}$ is explicitly chosen to be representative of *all* of the features of the integrand. Linearization around the same $\mathcal{L}$ further takes into account the behavior of the integrand perpendicular and close by to this manifold, which can be quite different from the representative whole, and frequently, this can lead to a worse approximation.

For completeness, we substitute in ξ and expand Eq. (5), revealing the full DHK formula as

$$\langle \Psi_\beta(0) \mid \Psi_\beta(t) \rangle_{\mathrm{DHK}} = \mathcal{N}^{-1} \int_{\mathcal{L}} \mathrm{d}l \mathcal{A}(l,t) g_\beta(l,0) g_\beta^*(l,t) e^{\frac{i}{\hbar} S(\boldsymbol{p}_0(l), \boldsymbol{q}_0(l), t)}, \tag{13}$$

where

$$g_\beta(l,0) = \exp\left[-\frac{1}{2} \frac{\gamma\gamma_\beta}{\gamma+\gamma_\beta} (\boldsymbol{q}_\beta - \boldsymbol{q}_0(l))^2 - \frac{1}{2\hbar^2(\gamma+\gamma_\beta)} (\boldsymbol{p}_\beta - \boldsymbol{p}_0(l))^2 + \frac{i}{\hbar(\gamma+\gamma_\beta)} (\boldsymbol{q}_0(l) - \boldsymbol{q}_\beta)(\gamma \boldsymbol{p}_\beta + \gamma_\beta \boldsymbol{p}_0(l)) \right], \tag{14}$$

$$g_\beta(l,t) = \exp\left[-\frac{1}{2} \frac{\gamma\gamma_\beta}{\gamma+\gamma_\beta} (\boldsymbol{q}_\beta - \boldsymbol{q}_t(l))^2 - \frac{1}{2\hbar^2(\gamma+\gamma_\beta)} (\boldsymbol{p}_\beta - \boldsymbol{p}_t(l))^2 + \frac{i}{\hbar(\gamma+\gamma_\beta)} (\boldsymbol{q}_t(l) - \boldsymbol{q}_\beta)(\gamma \boldsymbol{p}_\beta + \gamma_\beta \boldsymbol{p}_t(l)) \right], \tag{15}$$

$$\mathcal{A}(l,t) = \sqrt{\det\left[\frac{1}{2} \left(\frac{\partial \boldsymbol{p}_t(l)}{\partial \boldsymbol{p}_0(l)} + \frac{\partial \boldsymbol{q}_t(l)}{\partial \boldsymbol{q}_0(l)} - i\gamma\hbar \frac{\partial \boldsymbol{q}_t(l)}{\partial \boldsymbol{p}_0(l)} + \frac{i}{\hbar\gamma} \frac{\partial \boldsymbol{p}_t(l)}{\partial \boldsymbol{q}_0(l)} \right) \right]}, \tag{16}$$

and

$$\mathcal{N} = \int_{\mathcal{L}} \mathrm{d}l g(l,0) g^*(l,0). \tag{17}$$

γ_β is the dispersion of the initial Gaussian wavepacket and γ are those of the "frozen" sampling Gaussians over which the integration is performed.

FURTHER DISCUSSION

It is possible to gain further appreciation of the conditions necessary for DHK to achieve good accuracy by examining how DHK handles autocorrelations in a simpler hyperbolic system. As Fig. 4 shows, if a coherent state is placed on the saddle point of this system, DHK actually fails miserably (LHK becomes exact, as expected in a system that can be exactly linearized). On the other hand, if the coherent state is started displaced off of the saddle point, DHK fares far better (see Fig. 4). This can be explained by noting that the former produces no appreciable action gradient in the overlap region between the initial and final states and thus falls in the region of poor performance marked by ⊛ in Fig. 3, whereas the latter's gradient is angled almost perpendicular to its major axis (as seen in the insets of Fig. 4).

Unlike a "linearized" propagator, DHK relies on a one-dimensional integral that can best capture all the information of a higher dimensional phase space. When there is no modulating phase from the action, DHK's single integral will likely only perform well when the dynamics of the state are all captured by one parameter. A state in a hyperbolic system perched on top of the saddle-point sits there indefinitely while exhibiting *both* compression and stretching dynamics. On the other hand, a state displaced from the saddle point is instead mostly seen as translating away from the perspecitive of its initial state. The former dynamics would likely require at least two integrals to accurately capture if one of them is selected along the unstable manifold; the other would have to be chosen to take into account the compression dynamics. If we wish to have only one integral as in Eq. (5), both the compression and stretching dynamics need to be captured by the single manifold we choose. Therefore, we can perhaps imagine fixing DHK's inferior autocorrelation in this case by choosing $\mathcal{L}$ such that it lies equally along the stable and unstable manifolds, thereby equally capturing the dynamics of both stretching and compressing. Such a change produces the "corrected DHK" curve in Fig. 4. Though most systems would be difficult to treat in this way, this suggests that DHK's results may be improved for some states if a manifold not corresponding to the fastest growing one is chosen as its integral's domain.

CONCLUSIONS

Through a simple model of the dominant contributions to HK's integral during recurrences in one-dimensional systems, we showed what conditions are necessary for DHK's single integral to perform comparably when it is chosen to lie along the state's fastest growing manifold. In particular, we found that it generally works well as long as the action gradient during recurrences is not perpendicular to this manifold.

These conditions may also hold in more dimensions and may suggest why DHK often seems applicable in systems with greater than one dimension, though it remains to be verified that the trends discussed here remain true. It would be interesting to see if DHK's performance in many-dimensions, when $\mathcal{L}$ is chosen to be the fastest growing manifold of a state, is still contingent on the gradient of its action not lying perpendicular to $\mathcal{L}$. As we showed in our earlier Communication, DHK frequently works well in many-dimensional systems, so perhaps this is a limitation that is often sufficiently satisfied. For attempts at implementing DHK for coherent state autocorrelations in general systems that are at least quasi-periodic, we recommend the same method as the one used herein to find the best manifold $\mathcal{L}$ for DHK's integral domain; all the one-dimensional manifolds in Fig. 2 (over which the integration was performed in DHK) were chosen by examining the stability matrix of the state's central classical trajectory, determining when its eigenvalues became real and their magnitudes maximal near either the trajectory's first or second quasi-return to its initial point and choosing the associated eigenvector. This is the approach we found most success with and corresponds to approximately choosing the state's "fastest growing" manifold.

The formalism for DHK presented herein also suggests that the method can work quite well for anharmonic systems. In fact, the quartic potential examined in Fig. 1 illustrates how well DHK performs for a system with a potential containing no global quadratic terms at all. However, in general, the fastest growing manifold of such systems will not be linear and will exhibit some curvature since dynamics in higher than second order potentials are not completely described by linearizing their dynamics. This suggests that DHK may see improvement from selecting $\mathcal{L}$ to be a curved manifold. It would also be interesting to see how well DHK performs in chaotic or unbounded systems, where previous efforts in this direction have seen most improvement over HK (such as Filinov filtering).

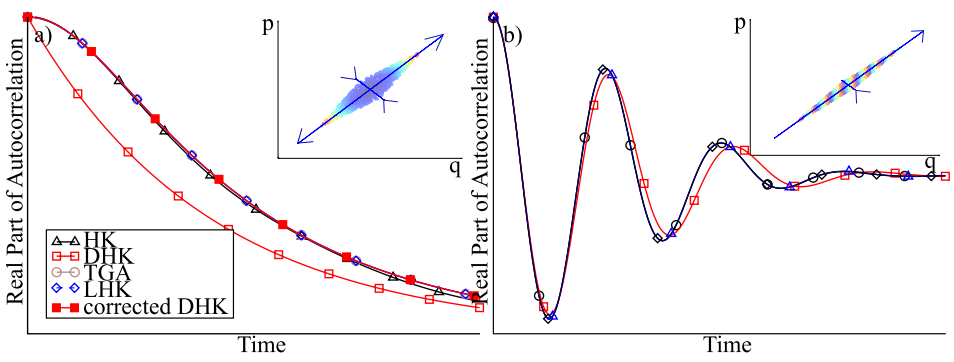

FIG. 4. The real part of the autocorrelation for a coherent state obeying hyperbolic dynamics initially situated (a) on the saddle point and (b) off the saddle point. When $\mathcal{L}$ is selected to be along the unstable manifold, DHK performs better in the latter case. If $\mathcal{L}$ is angled to lie equally along stable and unstable manifolds, DHK's performance improves in the former case (producing the "corrected DHK" curve).

ACKNOWLEDGMENTS

The authors thank the Faculty of Arts and Sciences and the Department of Chemistry and Chemical Biology at Harvard University for generous support of this work.

APPENDIX: DERIVATION OF SELECT FORMULAE

Derivation of LHK

We change the integration over phase space variables in HK to a new set $(l_0(\boldsymbol{q}_0,\boldsymbol{p}_0),\boldsymbol{n}_0(\boldsymbol{q}_0,\boldsymbol{p}_0))$, where l_0 lies along our chosen manifold and $\boldsymbol{n}_0$ are the remaining perpendicular degrees of freedom. The Jacobian of this transformation is equal to 1 since it is equivalent to just a rotation and translation of the $(\boldsymbol{p}_0,\boldsymbol{q}_0)$ variables.

We make an approximation by linearizing our action around $\boldsymbol{n}_0 = \boldsymbol{n}_\beta$ where $(l_\beta,\boldsymbol{n}_\beta) \equiv (\boldsymbol{p}_\beta,\boldsymbol{q}_\beta)$, and we define ζ to be the argument of the exponentials in Eq. (1) such that $g_\beta = \exp(\zeta)$,

$$\boldsymbol{u}(t) = \left[\left(\frac{\partial\zeta(\boldsymbol{p}_t(l_t,\boldsymbol{n}_t),\boldsymbol{q}_t(l_t,\boldsymbol{n}_t))}{\partial\boldsymbol{n}_0}\right)_{l_0}\right]_{\boldsymbol{n}_0=\boldsymbol{n}_\beta}, \tag{A1}$$

and

$$\boldsymbol{U}(t) = \left[\left(\frac{\partial^2\zeta(\boldsymbol{p}_t(l_t,\boldsymbol{n}_t),\boldsymbol{q}_t(l_t,\boldsymbol{n}_t))}{\partial\boldsymbol{n}_0^2}\right)_{l_0}\right]_{\boldsymbol{n}_0=\boldsymbol{n}_\beta}, \tag{A2}$$

so that we can express $g_\beta(\boldsymbol{p}(l_t,\boldsymbol{n}_t),\boldsymbol{q}(l_t,\boldsymbol{n}_t))$ more easily in terms of the new coordinates,

$$g_\beta(l_0,\boldsymbol{n}_0) = \exp\left\{\frac{1}{2}(\boldsymbol{n}_0-\boldsymbol{n}_\beta)\cdot\boldsymbol{U}(0)\cdot(\boldsymbol{n}_0-\boldsymbol{n}_\beta)^T + \boldsymbol{u}(0)\cdot(\boldsymbol{n}_0-\boldsymbol{n}_\beta)^T + \zeta\left(\boldsymbol{p}(l_0,\boldsymbol{n}_\beta),\boldsymbol{q}(l_0,\boldsymbol{n}_\beta)\right)\right\}, \tag{A3}$$

and

$$g^*_\beta(l_t,\boldsymbol{n}_0) = \exp\left\{\frac{1}{2}(\boldsymbol{n}_0-\boldsymbol{n}_\beta)\cdot\boldsymbol{U}^*(t)\cdot(\boldsymbol{n}_0-\boldsymbol{n}_\beta)^T + \boldsymbol{u}^*(t)\cdot(\boldsymbol{n}_0-\boldsymbol{n}_\beta)^T + \zeta^*(\boldsymbol{p}(l_t,\boldsymbol{n}_t),\boldsymbol{q}(l_t,\boldsymbol{n}_t))\,|_{\boldsymbol{n}_0=\boldsymbol{n}_\beta}\right\}. \tag{A4}$$

We also linearize the action,

$$S_t^{\mathrm{lin}}(\boldsymbol{p}_0,\boldsymbol{q}_0) = S_t^{\mathrm{lin}}(l_0,\boldsymbol{n}_0) \equiv S_t(l_0,\boldsymbol{n}_0=\boldsymbol{n}_\beta) + \left(\frac{\partial S_t}{\partial\boldsymbol{n}_0}\right)_{l_0}\Bigg|_{\boldsymbol{n}_0=\boldsymbol{n}_\beta}\cdot(\boldsymbol{n}_0-\boldsymbol{n}_\beta)^T \tag{A5}$$

$$+\frac{1}{2}(\boldsymbol{n}_0-\boldsymbol{n}_\beta)\cdot\left(\frac{\partial^2 S_t}{\partial\boldsymbol{n}_0^2}\right)_{l_0}\Bigg|_{\boldsymbol{n}_0=\boldsymbol{n}_\beta}\cdot(\boldsymbol{n}_0-\boldsymbol{n}_\beta)^T. \tag{A6}$$

We neglect all derivatives that are higher order than the stability matrix elements.

Hence, the integral becomes

$$\left\langle\Psi_\beta(0)|\Psi_\beta(t)\right\rangle_{\mathrm{HK}} \approx \left(\frac{\sqrt{\gamma\gamma_\beta}}{\pi\hbar\left(\gamma+\gamma_\beta\right)}\right)^N\int \mathrm{d}l_0\int \mathrm{d}\boldsymbol{n}_0 C_t(l_0,\boldsymbol{n}_0)g_\beta(l_0,\boldsymbol{n}_0)g^*_\beta(l_t,\boldsymbol{n}_0)\exp\left[iS_t^{\mathrm{lin}}(l_0,\boldsymbol{n}_0)/\hbar\right]. \tag{A7}$$

We perform the Gaussian integral over $\boldsymbol{n}_0$ linearized around $\boldsymbol{n}_\beta$ to obtain the LHK,

$$\left\langle\Psi_\beta(0)|\Psi_\beta(t)\right\rangle_{\mathrm{LHK}} = \int_{-\infty}^{\infty}\mathrm{d}l_0\int_{-\infty}^{\infty}\mathrm{d}\boldsymbol{n}_0\mathcal{N}(l_0)\exp\left[-\frac{1}{2}(\boldsymbol{n}_0-\boldsymbol{n}_\beta)\cdot\boldsymbol{A}(l_0,t)\cdot(\boldsymbol{n}_0-\boldsymbol{n}_\beta)^T + \boldsymbol{b}(l_0)\cdot(\boldsymbol{n}_0-\boldsymbol{n}_\beta)^T\right] \tag{A8}$$

$$= \int_{-\infty}^{\infty}\mathrm{d}l_0\mathcal{N}(l_0)\left(\frac{(2\pi)^{2N-1}}{\det\boldsymbol{A}(l_0,t)}\right)^{1/2}\exp\left(\frac{1}{2}\boldsymbol{b}(l_0,t)\cdot\boldsymbol{A}(l_0,t)^{-1}\cdot\boldsymbol{b}(l_0,t)^T\right), \tag{A9}$$

where

$$\boldsymbol{A}(l_0,t) = -\left[\boldsymbol{U}(0)+\boldsymbol{U}^*(t)+\frac{i}{\hbar}\left(\frac{\partial^2 S_t}{\partial\boldsymbol{n}_0^2}\right)_{l_0}\Bigg|_{\boldsymbol{n}_0=\boldsymbol{n}_\beta}\right], \tag{A10}$$

$$\boldsymbol{b}(l_0,t) = \left[\boldsymbol{u}(0)+\boldsymbol{u}^*(t)+\frac{i}{\hbar}\left(\frac{\partial S_t}{\partial\boldsymbol{n}_0}\right)_{l_0}\Bigg|_{\boldsymbol{n}_0=\boldsymbol{n}_\beta}\right], \tag{A11}$$

and

$$\mathcal{N}(l_0,\boldsymbol{n}_0) = \left(\frac{\sqrt{\gamma\gamma_\beta}}{\pi\hbar\left(\gamma+\gamma_\beta\right)}\right)^N C_t(\boldsymbol{p}_0(l_0),\boldsymbol{q}_0(l_0))e^{iS_t(l_0,\boldsymbol{n}_0=\boldsymbol{n}_\beta)/\hbar}$$

$$\times\exp\left\{\zeta(\boldsymbol{p}(l_0,\boldsymbol{n}_\beta),\boldsymbol{q}(l_0,\boldsymbol{n}_\beta)) + \zeta^*(\boldsymbol{p}(l_t,\boldsymbol{n}_t),\boldsymbol{q}(l_t,\boldsymbol{n}_t))\,|_{\boldsymbol{n}_0=\boldsymbol{n}_\beta}\right\}. \tag{A12}$$

Combining all of this together in one expression, we find

$$\begin{aligned}\langle\Psi_\beta(0)|\Psi_\beta(t)\rangle_{\mathrm{LHK}} = &\int_{-\infty}^{\infty} dl_0 \left(\frac{\sqrt{\gamma\gamma_\beta}}{\pi\hbar(\gamma+\gamma_\beta)}\right)^N C_t(\boldsymbol{p}_0(l_0,\boldsymbol{n}_0=\boldsymbol{n}_\beta),\boldsymbol{q}_0(l_0,\boldsymbol{n}_0=\boldsymbol{n}_\beta))\left(\frac{(2\pi)^{2N-1}}{\det \boldsymbol{A}(l_0,t)}\right)^{1/2} e^{iS_t(l_0,\boldsymbol{n}_0=\boldsymbol{n}_\beta)/\hbar}\\ &\times \exp\left\{\zeta(\boldsymbol{p}(l_0,\boldsymbol{n}_\beta),\boldsymbol{q}(l_0,\boldsymbol{n}_\beta)) + \zeta^*(\boldsymbol{p}(l_t,\boldsymbol{n}_t),\boldsymbol{q}(l_t,\boldsymbol{n}_t))\mid_{\boldsymbol{n}_0=\boldsymbol{n}_\beta}\right\}\\ &\times \exp\left(\frac{1}{2}\boldsymbol{b}(l_0,t)\cdot\boldsymbol{A}(l_0,t)^{-1}\cdot\boldsymbol{b}(l_0,t)^T\right). \end{aligned} \tag{A13}$$

Derivation of Eq. (8)

Suppose we start with a Gaussian $\Psi_\beta(q,0) = \left(\frac{\Re\gamma_0}{\pi}\right)^{\frac{1}{4}} \exp\left[-\frac{\gamma_0}{2}(q-q_\beta^2) + \frac{i}{\hbar}p_\beta(q-q_\beta)\right]$, where $\gamma_0 \in \mathbb{R}$ (a coherent state) and we are interested in its return to overlap itself at (p_β, q_β) at some time t. We consider the case that the state has remained a Gaussian but has acquired a new dispersion $\gamma_t \in \mathbb{C}$ (i.e., the state may now be rotated and squeezed with respect to its initial state). If this Gaussian's major axis is rotated with respect to the p- or q-axis then $\Delta q\Delta p = \frac{\hbar}{2}\sqrt{1+\frac{\Re\gamma_t^2}{\Im\gamma_t^2}} > \frac{\hbar}{2}$. This corresponds to a Gaussian aligned with some major and minor axes rotated by θ to the p,q-axes in whose frame $\Im\gamma = 0$. It can be shown[11] that

$$\Re\gamma_t = \frac{\gamma}{d(\theta)}, \tag{A14}$$

$$\Im\gamma_t = \frac{(1-\gamma^2\hbar^2)\sin\theta\cos\theta}{\hbar d(\theta)}, \tag{A15}$$

where

$$d(\theta) = \cos^2\theta + \gamma^2\hbar^2\sin^2\theta. \tag{A16}$$

If $\gamma = \frac{1}{\hbar}$, then the Gaussian appears to be a circle in phase space. For $\gamma > \frac{1}{\hbar}$ ($\gamma < \frac{1}{\hbar}$), its major axis corresponds to the p-axis (q-axis) in the rotated frame.

The Wigner transform of these Gaussians is

$$\rho_W(p,q) = \frac{1}{2}\int_{-\infty}^{\infty} ds \Psi_\beta\left(q-\frac{s}{2},t\right)\Psi_\beta^*\left(q+\frac{s}{2},t\right)\exp\left(\frac{i}{\hbar}sp\right) \tag{A17}$$

$$= \exp\left[-\gamma_t\left(2-\frac{\gamma_t}{\Re\gamma_t}\right)(q-q_\beta)^2 - \frac{(p-p_\beta)^2}{\hbar^2\Re\gamma_t} + \frac{2i}{\hbar}\left(\frac{\gamma_t}{\Re\gamma_t}-1\right)(q-q_\beta)(p-p_\beta)\right]. \tag{A18}$$

Using Eqs. (A14) and (A15), this can be reexpressed in a more intuitive form as Eq. (8).

Parameters

All results were obtained with $\hbar = 1$. We express all quantities below as defined in Eqs. (13)-(17).

For the quartic oscillator results, the mass was $m = 0.979\,573$, the potential was $V = \omega q^4$, with $\omega = 2\,012\,640.0$. The states A-D all had dispersions $\gamma_\beta = \gamma = \frac{1.0}{0.042\,561\,5^2}$. In particular, for A, $(p_\beta, q_\beta) = (0.0, 0.4)$, $\mathcal{L} = (-0.999\,997\,388, 0.002\,285\,810\,84)$, and the time step $\delta t = 0.000\,02$; for B, $(p_\beta, q_\beta) = (240.0, 0.0)$, $\mathcal{L} = (0.999\,999\,993, 0.000\,114\,148\,579)$, and $\delta t = 0.000\,02$; for C, $(p_\beta, q_\beta) = (0.0, 0.1)$, $\mathcal{L} = (0.999\,832\,662, -0.018\,293\,386\,2)$, and $\delta t = 0.000\,04$; and for D, $(p_\beta, q_\beta) = (80.0, 0.0)$, $\mathcal{L} = (0.999\,999\,997, 0.000\,074\,317\,050\,1)$, and $\delta t = 0.000\,04$.

For the inverted oscillator results, the mass was $m = 1$ and the potential was $V = -m\omega^2 q^2$ with $\omega = 1.0$. The dispersion was $\gamma_\beta = \gamma = 1.0$. The time step was $\delta t = 0.0005$. The state displaced off the saddle point began at $(p_\beta, q_\beta) = (0.0, 10.0)$.

[1] E. J. Heller, "Frozen Gaussians: A very simple semiclassical approximation," J. Chem. Phys. **75**(6), 2923–2931 (1981).
[2] M. F. Herman and E. Kluk, "A semiclasical justification for the use of non-spreading wavepackets in dynamics calculations," Chem. Phys. **91**(1), 27–34 (1984).
[3] K. G. Kay, "Integral expressions for the semiclassical time-dependent propagator," J. Chem. Phys. **100**(6), 4377–4392 (1994).
[4] K. G. Kay, "Numerical study of semiclassical initial value methods for dynamics," J. Chem. Phys. **100**(6), 4432–4445 (1994).
[5] E. J. Heller, "Cellular dynamics: A new semiclassical approach to time-dependent quantum mechanics," J. Chem. Phys. **94**(4), 2723–2729 (1991).
[6] H. Wang, D. E. Manolopoulos, and W. H. Miller, "Generalized filinov transformation of the semiclassical initial value representation," J. Chem. Phys. **115**(14), 6317–6326 (2001).
[7] K. G. Kay, "Semiclassical propagation for multidimensional systems by an initial value method," J. Chem. Phys. **101**(3), 2250–2260 (1994).
[8] M. Spanner, V. S. Batista, and P. Brumer, "Is the filinov integral conditioning technique useful in semiclassical initial value representation methods?," J. Chem. Phys. **122**(8), 084111 (2005).
[9] S. M. Anderson, D. Neuhauser, and R. Baer, "Trajectory-dependent cellularized frozen Gaussians, a new approach for semiclassical dynamics: Theory and application to He–naphtalene eigenvalues," J. Chem. Phys. **118**(20), 9103–9108 (2003).
[10] L. Kocia and E. J. Heller, "Communication: HK propagator uniformized along a one-dimensional manifold in weakly anharmonic systems," J. Chem. Phys. **141**(18), 181102 (2014).
[11] E. J. Heller, "Chaos and quantum physics," in *Les Houches Summer School Session I, II* (North-Holland, 1991).